Neural Bases of Cognitive ERPs: More than Phase Reset

Juergen Fell[1], Thomas Dietl[1], Thomas Grunwald[1,2], Martin Kurthen[1],
Peter Klaver[1], Peter Trautner[1], Carlo Schaller[1], Christian E. Elger[1],
and Guillén Fernández[1,3]

Abstract

■ Up to now, two conflicting theories have tried to explain the genesis of averaged event-related potentials (ERPs): Whereas one hypothesis claims that ERPs originate from an event-related activation of neural assemblies distinct from background dynamics, the other hypothesis states that ERPs are produced by phase resetting of ongoing oscillatory activity. So far, this question has only been addressed for early ERP components. Late ERP components, however, are generally thought to represent superimposed activities of several anatomically distinct brain areas. Thus, the question of which mechanism underlies the genesis of late ERP components cannot be easily answered based on scalp recordings. In contrast, two well-investigated late ERP components recorded invasively from within the human medial temporal lobe (MTL) in epilepsy patients, the so-called MTL-P300 and the anterior MTL-N400 (AMTL-N400), are based on single source activity. Hence, we investigated whether the MTL-P300 and the AMTL-N400 are based on an event-related activity increase, a phase reset of ongoing oscillatory activity or both. ERPs were recorded from the hippocampus and rhinal cortex in subjects performing a visual oddball paradigm and a visual word recognition paradigm. With wavelet techniques, stimulus-related phase-locking and power changes were analyzed in a frequency range covering 2 to 48 Hz. We found that the MTL-P300 is accompanied by both phase reset and power increase and that both effects overlap partly in time. In contrast, the AMTL-N400 is initially associated with phase locking without power increase and only later during the course of the AMTL-N400 we observed an additional power increase. In conclusion, both aspects, event-related activation of neural assemblies and phase resetting of ongoing activity seem to be involved in the generation of late ERP components as recorded in cognitive tasks. Therefore, separate analysis of event-related power and phase-locking changes might reveal specific insights into the mechanisms underlying different cognitive functions. ■

INTRODUCTION

Recently, the debate (e.g., Sayers, Beagley, & Henshall, 1974; Basar, 1972, 1980) has been reinitiated, whether event-related potential (ERP) components result from a stimulus-induced increase in EEG power or from phase locking of ongoing EEG activity, that is, a stimulus-related concentration of phases (Makeig et al., 2002). In theory, both aspects can contribute to the generation of a component, which later appears in the ERP average (e.g., Sannita et al., 2001; Demiralp, Ademoglu, Istefanopulos, & Gulcur, 1998; Yordanova & Kolev, 1998; Basar, Basar-Eroglu, Rosen, & Schutt, 1984). Stimulus-induced power changes are thought to correspond to the event-related activation of a neural assembly distinct from ongoing background dynamics. On the other hand, phase resetting of ongoing oscillatory activity can produce an ERP component without changes in the amount of activated neurons. In this case, a functional imaging approach like fMRI would not find a related activation, because no net change in regional neural activity occurs. Therefore, the clarification of the question at issue here might not only explain the biological basis of cognitive operations in more detail, it might also explain in part discrepancies between studies using EEG or functional imaging approaches like fMRI.

Based on a recent investigation, it has been reported that the average N100 component in a visual selective attention task is mainly produced by stimulus-related phase resetting of ongoing EEG activity, and power changes played a negligible role (Makeig et al., 2002). However, the absence of a prominent event-related increase of EEG power at the dominant frequency of the ERP has not been rigorously demonstrated in this study. But, it even may be the case that an ERP component is observed solely due to phase locking and in spite of a poststimulus decrease in EEG power (Fell, Hinrichs, & Röschke, 1997). Up to now, it nevertheless has remained an open question whether the predominance of phase resetting is a general mechanism for all and not only for early ERP components. For instance, in case of late ERP components like the P300 or the N400,

[1]University of Bonn, Germany, [2]Swiss Epilepsy Centre, Zurich, Switzerland, [3]F.C. Donders Center for Cognitive Neuroimaging, Nijmegen, The Netherlands

stimulus-induced changes in EEG power might contribute significantly to the average ERP.

In the present study, we thus analyzed how phase-locking and power changes contribute differentially to the generation of the medio-temporal P300 (MTL-P300) and the anterior medio-temporal N400 (AMTL-N400) (i.e., typical late ERP components). MTL-P300 and AMTL-N400 were recorded via depth electrodes from the healthy hemisphere in patients with unilateral temporal lobe epilepsy, who performed a visual oddball and a continuous visual word recognition experiment. Similar to the surface P300, the MTL-P300 is elicited by rare target stimuli in auditory or visual "oddball" paradigms. In contrast to multiple sources underlying the widespread surface P300, the MTL-P300 (e.g., Halgren, Marinkovic, & Chauvel, 1998), which actually represents a negative deflection, is generated locally within the hippocampus proper (e.g., Grunwald, Beck, et al., 1999; Halgren, Squires, et al., 1980). Although its functional significance is not yet clear, the MTL-P300 is probably associated with the hippocampal contribution to updating or closure of a context within working memory (Verleger, 1998; Donchin & Coles, 1988). The AMTL-N400 is found after visual word presentation similar to the broadly distributed surface N400 (Halgren & Smith, 1987). The source of the AMTL-N400, which seems to be correlated with semantic operations supporting declarative memory indirectly (Fernández, Klaver, Fell, Grunwald, & Elger, 2002; Fernández et al., 1999; Nobre & McCarthy, 1995), could be localized within the rhinal, probably perirhinal, cortex (McCarthy, Nobre, Bentin, & Spencer, 1995). Like the surface N400, the AMTL-N400 is reduced in amplitude after repeated presentation of a certain word (e.g., Grunwald, Lehnertz, Heinze. Helmstaedter, & Elger, 1998; Smith, Stapleton, & Halgren, 1986).

Compared to the analysis of surface-recorded P300 and N400 components, the analysis of the depth-recorded MTL-P300 and AMTL-N400 offers a major advantage. In intracranial recordings, polarity inversions and steep voltage gradients over small distances were observed for these components, which indicate that the sources of the MTL-P300 and the AMTL-N400 are narrowly circumscribed (McCarthy et al., 1995; Halgren, Squires, et al., 1980). In other words, the MTL-P300 and the AMTL-N400 appear to have single, localized generators (of course, with some spatial extension; Fernández, Heitkemper, et al., 2001). Hence, phase-locking and amplitude contributions can be analyzed at the locus of ERP generation and are not influenced by multiple projections of P300 and N400 generators to different scalp positions. In particular, it is impossible to distinguish phase-locking and amplitude changes from local phase and amplitude synchronization of neighboring cortex regions based on surface EEG data (e.g., Menon et al., 1996; Bullock et al., 1995). On the other hand, the analysis of depth-recorded MTL-P300 and AMTL-N400

has been shown to allow the investigation of local EEG characteristics, which are practically not influenced by volume conduction of activity from other limbic regions (e.g., McCarthy et al., 1995). Thus, the objective of the present investigation was to reveal reliable information about the specific contribution of amplitude and phase-locking effects to the generation of late ERP components by focusing on the two best investigated, intracranially recorded late ERP components, the MTL-P300 and the AMTL-N400.

If an ERP component was solely based on phase locking of ongoing oscillatory EEG activity one would expect an increase in phase synchronization but not in power. In this strict version of phase resetting, a local stimulus-related activation of neurons may not be denied, but this response would not add EEG power in frequencies relevant to the ERP in question. If, however, an ERP component was solely based on an event-related activity increase, one would expect a power enhancement, which is probably associated with an increase in intertrial phase locking depending on the amount of phase locking of the additional activity. If the additional activity was not phase locked at all, it would not contribute to the averaged ERP component. In case of a power enhancement and a simultaneous phase-locking increase, which is likely in the evoked model, it is therefore not possible to unambiguously distinguish the phase-locking increase due to additional, more or less phase-locked activity from the phase reset of ongoing activity. But, even if there is both phase-locking and power increase at the frequencies relevant to the ERP component, these aspects may be dissociable in time. In any case, the approach described here enables us to validate or invalidate the hypothesis that late ERP components like the MTL-P300 or the AMTL-N400 are solely based on phase resetting of ongoing oscillatory EEG activity as previously suggested for early ERP components (Makeig et al., 2002).

In brief, for both paradigms, EEG trials were wavelet transformed in the frequency range from 2 to 48 Hz and from the transformed data power and phase-locking values were calculated (see Methods). Power and phase-locking values were averaged for non-overlapping successive time windows of 100 msec duration from −200 to 1000 msec and were normalized with respect to the prestimulus window from −200 to −100 msec. For graphical depiction, power and phase-locking values were transformed into dB scale. We conducted three-way ANOVAs with time (window) and stimulus (target vs. nontarget, hits [correctly recognized old items] vs. correct rejections [correctly identified new items]) as repeated measures, and frequency as independent variable. Two-way ANOVAs were calculated separately for target and nontarget responses in the oddball paradigm and hits and correct rejections in the recognition paradigm. Subsequently, two-tailed paired-sample t tests comparing target and nontarget responses, as well as

hits and correct rejections, were performed for each individual time window and frequency.

RESULTS

Behavioral Results

In the oddball paradigm, patients correctly identified 96.3 ± 3.2% of the target stimuli and gave 0.4 ± 0.7% false alarms in response to nontarget stimuli. In the continuous recognition experiment, 67.5 ± 19.6% of the old words were correctly identified and 78.4 ± 19.1% of the new words were correctly rejected.

## MTL-P300: Average ERP Waveforms

The average MTL-P300 waveforms recorded from within the hippocampus elicited by correctly identified target compared to nontarget stimuli are shown in Figure 1. In

line with previous reports (e.g., Grunwald, Beck, et al., 1999; Halgren, Squires, et al., 1980), target stimuli were associated with a marked negative potential peaking around 460 msec after stimulus onset. Across all patients, mean peak amplitudes ($\pm SD$) of the hippocampal P300 component were −104 (74) μV, mean latencies were 458 (69) msec. For nontarget stimuli only comparatively small negative waveforms were recorded with amplitudes of about 20 μV and peak latencies of around 300 msec after stimulus onset.

MTL-P300: Phase Locking

We observed for target responses a phase-locking increase of delta activity in the P300 and post-P300 time range. On the other hand, nontarget responses showed a bias of phase locking toward alpha and theta frequencies. The timing of the phase-locking increase for target

Figure 1. Top: Averaged ERPs recorded from within the hippocampus (MTL-P300) for target and nontarget responses in a visual oddball paradigm. Below: Phase-locking and power changes associated with the MTL-P300 recorded from within the hippocampus proper. The plots show color-coded phase-locking and power values, which have been normalized with respect to a prestimulus baseline (−200 to 100 msec) and have been transformed into dB scale ($10*\log_{10}$). The different frequencies (2 to 48 Hz) are represented in the *y*-direction, while time relative to the onset of letter presentation is depicted in the *x*-direction.
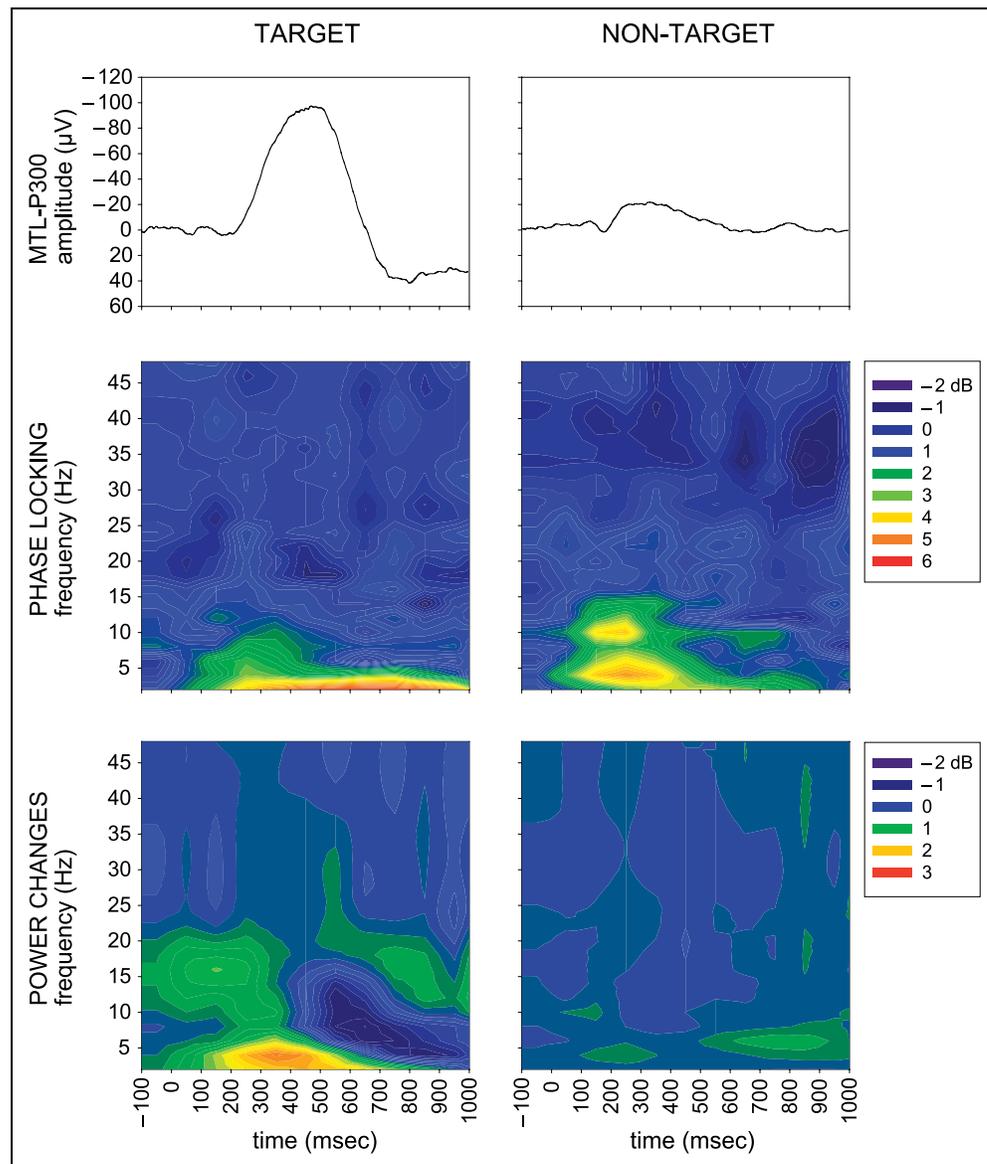
responses comprises the negative deflection of the MTL-P300 plus the subsequent positive deflection in the averaged ERPs. ANOVA revealed main effects for the factors time [$p < .0001$, $F(10,2640) = 13.66$, $\varepsilon = .511$] and frequency [$p < .0001$, $F(23,264) = 7.73$], as well as a significant Stimulus $\times$ Time $\times$ Frequency interaction [$p < .0001$, $F(230,2640) = 13.66$, $\varepsilon = .503$]. In detail, target responses showed a pronounced increase of phase locking of delta activity by up to around 6dB in the time range from 300 to 1000 msec [see Figure 1; main effect for time: $p = .0002$, $F(10,2640) = 5.58$, $\varepsilon = .413$, and a Time $\times$ Frequency interaction: $p < .0001$, $F(230,2640) = 2.87$, $\varepsilon = .413$]. Meanwhile, nontarget responses exhibited an earlier phase-locking increase of theta and alpha activity by up to 5 dB in the time range from 100 to 400 msec [main effect for time: $p < .0001$, $F(10,2640) = 12.10$, $\varepsilon = .497$, and a Time $\times$ Frequency interaction: $p < .0001$, $F(230,2640) = 2.34$, $\varepsilon = .497$]. t Tests yielded significant differences in phase locking between target and nontarget responses mainly around 2 Hz in the time range from 500 to 1000 msec (each $p < .05$), and around 10 Hz in the time range from 100 to 300 msec (each $p < .05$).

MTL-P300: Power Changes

Although we recognized an increase of delta and theta power in the P300 time range for target responses, no power enhancement was found for nontarget responses. The timing of the power increase for target responses seems to correspond to the timing of the negative deflection of the MTL-P300 in the averaged ERPs. We detected main effects for the factors time [$p < .0001$, $F(10,2640) = 20.40$, $\varepsilon = .432$] and frequency [$p < .05$, $F(23,264) = 1.73$], as well as a significant Stimulus $\times$ Time $\times$ Frequency interaction [$p < .0001$, $F(230,2640) = 2.26$, $\varepsilon = .409$]. In detail, target responses exhibited a clear increase of delta and theta power by up to 3 dB in the time range from 200 to 500 msec and a subsequent decrease of theta and alpha power by up to -2 dB in the time range from 500 to 1000 msec [see Figure 1; main effect for time: $p < .0001$, $F(10,2640) = 24.07$, $\varepsilon = .415$, and a Time $\times$ Frequency interaction: $p < .0001$, $F(230,2640) = 3.67$, $\varepsilon = .415$]. Nontarget responses, on the other hand, exhibited no significant power increase or decrease [neither a main effect for time, $F(10,2640) = 2.23$, $\varepsilon = .255$, nor a Time $\times$ Frequency interaction, $F(230,2640) = 1.19$, $\varepsilon = .255$]. t Tests yielded significant power differences between target and nontarget responses mainly around 2 Hz (0 to 600 msec, each $p < .05$), and subsequently mainly around 6 Hz (500 to 900 msec, each $p < .05$).

AMTL-N400: Average ERP Waveforms

The average AMTL-N400 waveforms recorded from the rhinal cortex elicited by hits (correctly recognized old words) and correct rejections (correctly identified new words) are shown in Figure 2. Within the rhinal cortex correct rejections were associated with a pronounced negative potential peaking around 430 msec after stimulus onset. Across all patients, mean peak amplitudes ($\pm SD$) of the AMTL-N400 component were -56 (34) μV, mean peak latencies were 427 (105) msec. Hits elicited comparatively smaller and earlier negative waveforms with amplitudes reaching -49 (34) μV and peaking at 386 (105) msec (paired two-tailed t tests: $t_7 = 2.77$, $p < .05$ and $t_7 = 3.12$, $p < .05$).

AMTL-N400: Phase Locking

Both correct rejections, as well as hits, exhibited phase-locking increases in the N400 time range. In parallel to the ERP amplitudes, phase-locking changes were more pronounced for correct rejections than for hits. For hits the timing of the phase-locking increase seems to comprise the AMTL-N400 component plus the subsequent positive deflection in the averaged ERPs. On the other hand, for correct rejections the center of the phase-locking response seems to correspond to the rising edge of the averaged AMTL-N400 component. ANOVA revealed main effects for the factors time [$p < .0001$, $F(10,1680) = 8.96$, $\varepsilon = .536$] and frequency [$p < .0001$, $F(23,168) = 4.18$], as well as a significant Stimulus $\times$ Time $\times$ Frequency [$p < .0001$, $F(230,1680) = 1.83$, $\varepsilon = .665$] interaction. In detail, correct rejections elicited a pronounced increase of phase locking of theta activity by up to around 7dB in the time range from 100 to 400 msec, which is followed by a decrease of phase locking of alpha activity by up to -2 dB in the time range between 500 and 900 msec [see Figure 2; main effect for time: $p < .0001$, $F(10,1680) = 19.73$, $\varepsilon = .537$, and a Time $\times$ Frequency interaction: $p < .0001$, $F(230,1680) = 2.40$, $\varepsilon = .537$]. Hits elicited a phase-locking increase of alpha activity by up to 5 dB in the time range between 100 and 300 msec and afterwards a phase locking increase of delta activity in the time range between 300 and 600 msec [main effect for time: $p < .0001$, $F(10,1680) = 9.73$, $\varepsilon = .500$, and a Time $\times$ Frequency interaction: $p = .0003$, $F(230,1680) = 1.58$, $\varepsilon = .500$]. t Tests yielded differences in phase locking between responses elicited by hits and correct rejections around 10 Hz in the time range from 600 to 900 msec (each $p < .1$).

AMTL-N400: Power Changes

An event-related power enhancement was found for correct rejections as well as for hits in the late N400 and post-N400 time range. In contrast to phase-locking changes, the power increase was more pronounced for hits than for correct rejections. For both hits and correct rejections, power increases mainly occur within time

Figure 2. Top: Averaged ERPs recorded from within the rhinal cortex (AMTL-N400) for hits (correctly recognized old words) and correct rejections (correctly identified new words) in a continuous visual word recognition paradigm. Below: Phase-locking and power changes associated with the AMTL-N400 recorded from within the rhinal cortex. The plots show color-coded phase-locking and power values, which have been normalized with respect to a prestimulus baseline (−200 to 100 msec) and have been transformed into dB scale ($10*\log_{10}$). The different frequencies (2 to 48 Hz) are represented in the y-direction, while time relative to the onset of word presentation is depicted in x-direction.
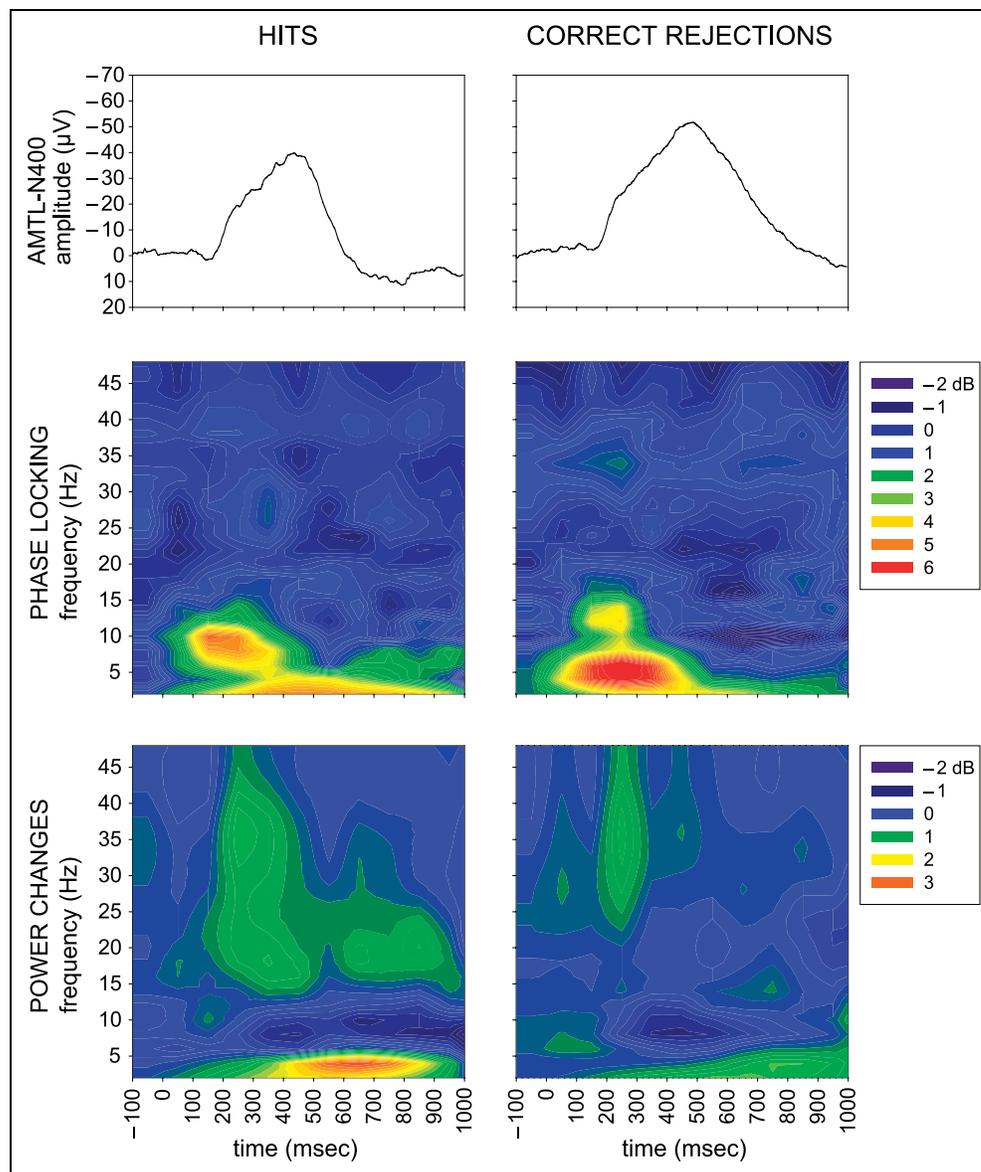
ranges succeeding the peaks of the AMTL-N400 components in the averaged ERPs. Main effects were detected for the factors time [$p < .0001$, $F(10,1680) = 7.11$, $\varepsilon = .399$] and frequency [$p < .01$, $F(23,168) = 2.09$], as well as a significant Stimulus × Time × Frequency [$p < .01$, $F(230,1680) = 1.40$, $\varepsilon = .564$] interaction. In detail, correct rejections exhibited an increase of delta and theta power by up to 2 dB in the time range from 400 to 1000 msec [see Figure 2; main effect for time: $p < .0001$, $F(10,1680) = 12.56$, $\varepsilon = .552$, and a Time × Frequency interaction: $p < .0001$, $F(230,1680) = 1.68$, $\varepsilon = .552$]. Compared to correct rejections, hits elicited a stronger increase of delta and theta power reaching up to 3 dB in the time range from 500 to 800 msec [main effect for time: $p < .0001$, $F(10,1680) = 13.30$, $\varepsilon = .442$, and a Time × Frequency interaction: $p < .0001$, $F(230,1680) = 2.19$, $\varepsilon = .442$]. Moreover, for both hits and correct rejections, power increases in the gamma

range reaching up to 1.5 dB mainly in the time range from 200 to 400 msec were observed. These power increases mainly seem to reflect induced gamma activity, as they were not accompanied by equivalent phase locking. t Tests yielded power differences between responses elicited by correct rejections and hits mainly around 2 Hz (300 to 500 msec, each $p < .1$) and 4 Hz (400 to 800 msec, each $p < .1$).

DISCUSSION

The present study aimed to investigate two competing hypotheses for the genesis of average ERPs focusing on late ERP components. One hypothesis claims that ERPs originate from a specific activation of neural assemblies distinct from background dynamics, which are regarded as stationary noise, resulting in a stimulus-related power

increase (e.g., Lopes da Silva, 1993). The other hypothesis states that ERPs are solely produced by a phase resetting of ongoing neural activity. Evidence for the validity of the second hypothesis has recently been reported for the visual N100 (Makeig et al., 2002). Here, we analyzed typical late ERP components, the MTL-P300 and the AMTL-N400, based on depth recordings from within the MTL. Because we directly recorded from within those structures, which are known to represent the sources of the MTL-P300 and the AMTL-N400, the hippocampus and the rhinal cortex, we were able to avoid that phase-locking and power analyses were influenced by the projection of several sources to different recording positions. In particular, phase-locking and amplitude changes as evaluated from surface recordings are not independent from phase and amplitude synchronization of the contributing cortex regions (e.g., Menon et al., 1996; Bullock et al., 1995). For example, if two sources are mutually antiphasic with respect to a certain surface position, the power as recorded from that surface position will be reduced compared to the total power of both source signals. On the other hand, the phase-locking values calculated for the surface position do not only depend on the degree of phase locking of both source signals, but also on their amplitude variations. And, of course, the choice of the surface position will strongly affect both power and phase-locking estimates.

Our findings based on depth recordings indicate that the MTL-P300 response to target stimuli is produced by both stimulus-related phase-locking and power changes. Hence, the results for the MTL-P300 support the stimulus-evoked model, but cannot rule out a possible contribution from phase resetting of ongoing activity. However, the AMTL-N400 might, at least initially, be based on phase reset only. Later during the course of the AMTL-N400 an additional power increase can be observed. Thus, our data invalidate the hypothesis that late ERP components are generated solely by a phase reset of ongoing ''background'' activity. On the other hand, for both MTL-P300 and AMTL-N400, the time course and frequency distribution of the phase-locking effects differ markedly from the power changes and both aspects only partly overlap. This finding suggests that MTL-P300 and AMTL-N400 cannot solely be ascribed to additional activations that are phase locked with respect to the stimuli. Instead, both mechanisms distinct activation of neural assemblies and phase reset of ongoing activity, seem to be involved in the generation of late ERPs. However, the nontarget response in the oddball paradigm may be regarded as an example of a potential, which is almost exclusively based on phase reset.

Although an enhancement of EEG power is thought to correspond to an activation of a larger amount of neural assemblies (e.g., Lopes da Silva, 1993), the interpretation of increased intertrial phase locking is less obvious. First of all, an increase of phase locking may indicate that the timing of stimulus processing exhibits less intertrial variability, as increased phase locking corresponds to a decreased variability of ERP latency. However, it is yet an open question whether intertrial phase locking may also have some functional significance related to single events. It has been suggested that slow ERP components like the CNV provide a threshold controlling the excitability of cortical networks (Elbert & Rockstroh, 1987). This model has also been proposed to be extendable to late ERP components like the P300 (e.g., Schupp, Lutzenberger, Rau, & Birbaumer, 1994). According to this interpretation, precise timing of the phase of a late ERP component could reflect that inhibition or facilitation of neural firing occurs exactly at the right time point within the processing sequence. In this sense, intertrial phase locking could have some relevance for single events, although this idea is yet rather speculative.

Another crucial question is in how far both ERP aspects, intertrial phase-locking and power changes, are visible in functional imaging based on hemodynamic responses. Recently, it has been shown that the blood oxygen level-dependent (BOLD) fMRI response is more closely correlated to local field potentials than to single- or multi-unit spike activity (Logothetis, 2002; Logothetis, Pauls, Augath, Trinath, & Oeltermann, 2001). Thus, there is good evidence that fMRI signals are more correlated to EEG and ERP activity than to neural firing of action potentials. However, phase shifts in the ERP response will only have a negligible influence on the phases of the BOLD responses because of the different time scales of ERP and fMRI signals. Thus, it must be assumed that the fMRI signal is correlated to ERP power changes, but rather not to phase-locking changes. However, even in case of a strict version of phase resetting, detection of a local hemodynamic change reflecting a local increase of neural activity, which does not add power at the level of summed field potentials, may be possible. On the other hand, failure of fMRI to detect a local hemodynamic change can rely on several reasons such as a too small volume of activation, susceptibility artifacts, or an inadequate signal-to-noise ratio. Here, we have demonstrated that both power and phase-locking effects distinctly contribute to the genesis of late ERP components. Therefore, the comparison between source analyses based on averaged ERPs and fMRI findings should be regarded with caution. Among others, one reason for discrepancies in source localizations may be that averaged ERPs also comprise intertrial phase-locking changes, which are not correlated to fMRI signal changes. Of course, this issue deserves further investigation. In conclusion, our findings suggest that separate analysis of event-related power and phase-locking changes can reveal better insight into distinct functional aspects underlying the genesis of late ERPs. We think that such an approach is

particularly advisable when ERP source analyses are integrated with imaging data.

METHODS

Subjects

MTL-P300

Twelve patients with pharmacoresistant temporal lobe epilepsy (9 women, 3 men, mean age: 40.3 ± 11.6 years) participated in this study. All 12 patients had unilateral seizure onset zones. In seven patients, the morphological correlate of the primary epileptogenic focus was found to be hippocampal sclerosis, five patients had unilateral lateral or medial temporal lesions like benign tumors or vascular malformations. In all patients, a local ictal onset pattern could be identified: MTL seizures originated always in the right MTL in six patients and always in the left MTL in the other six patients.

AMTL-N400

Eight patients with pharmacoresistant, unilateral temporal lobe epilepsy (3 women, 5 men, mean age: 41.9 ± 10.6 years) who did not participate in the oddball task participated in this part of the study. Three patients had hippocampal scleroses, in five patients we found other benign MTL lesions like cortical dysplasias. In four patients, seizures originated always in the right MTL; in the other four patients, seizures originated always in the left MTL.

Depth Electrodes

Bilateral, multicontact depth electrodes were inserted using a previously described technique (Van Roost, Solymosi, Schramm, Van Oosterwyck, & Elger, 1998) because the seizure onset zone could not be determined unequivocally for resective surgery by noninvasive means. The location of electrode contacts was ascertained by magnetic resonance images (MRI) in each patient. Contacts were mapped by transferring their positions from MRI to standardized anatomical drawings (Jackson & Duncan, 1996). MRI scans were acquired in the sagittal and adjusted coronal planes, perpendicular to the longitudinal axis of the hippocampus (repetition time = 3719 msec, echo time = 120 msec, flip angle = 90°, field of view = 22 cm; thickness: 2.0 mm; gap: 0.3 mm; 1.5 T) (ACS-II, Philips, Eindhoven, Netherlands).

Only EEG recordings from the MTL contralateral to the zone of seizure origin were analyzed in the present study to reduce poorly controllable effects introduced by the epileptic process (Grunwald, Elger, Lehnertz, Van Roost, & Elger, 1995). If seizures are proved to originate unilaterally, electrodes in the healthy MTL enable recordings of quasi-normal brain activity unrelated to epilepsy (Paller, McCarthy, Roessler, Allison, & Wood,

1992). Unilateral seizure onset was indicated in each patient by the fact that all seizures originated exclusively in depth recordings of one MTL.

At the time of the experiment, all patients were under stable anticonvulsive medication without benzodiazepines, barbiturates or phenytoin, that is, anticonvulsive drugs known to affect oscillatory EEG activity. No seizure occurred within 24 hours before the experiment. The ERP study was part of the presurgical workup providing predictors for seizure control and memory performance following surgical intervention (Grunwald, Lehnertz, Pezer, et al., 1999; Grunwald, Lehnertz, Helmstaedter, et al., 1998). It was approved by the local medical ethics committee and each patient gave written informed consent.

Experimental Paradigms

MTL-P300

In a visual oddball paradigm, two letters (white against black background) were presented randomly intermixed in central vision (horizontal visual angle 3.0°). The letter "x" was presented as a frequent stimulus with a probability of 80% and the letter "o" as the rare stimulus with 20% probability. A total of 300 stimuli was presented, each for a duration of 300 msec. The interstimulus interval varied randomly from 1000 to 1400 msec (mean 1200 msec). Patients faced the presentation monitor from around 80 cm distance sitting upright in an adjustable bed. They were asked to respond to each rare stimulus by pressing the button of a computer mouse.

AMTL-N400

In a continuous visual word recognition paradigm (Rugg & Nagy, 1989), 300 common German nouns were presented sequentially in uppercase letters (white against black background), in central vision (horizontal visual angle 3.0°), and for a duration of 200 msec (randomized interstimulus interval: mean: 1800 msec, range: 1400–2200 msec). Half of these words were repeated after 3 ± 1 (early) or 14 ± 4 (late) intervening stimuli. Patients were asked to indicate whether an item was new or old by pressing one of two buttons of a computer mouse in their dominant hand. Because earlier studies have revealed no reliable differences between MTL-ERPs to early and late repetitions (Grunwald, Lehnertz, Heinze, et al., 1998; Guillem, Elger, Lehnertz, Van Ross, & Elger, 1995), averages were collapsed across both lags for the present analysis.

EEG Recording

Depth electroencephalograms were referenced to linked mastoids, bandpass-filtered (0.01 Hz [6 dB/octave] to 70 Hz [12 dB/octave]), and recorded with a

sampling rate of 200 Hz. For the present analyses recordings from the nonpathological hemispheres were selected as described above. EEG trials were visually inspected for artifacts and around 5 % of all trials were excluded from analysis (e.g., epileptiform spikes). For each patient, one hippocampal electrode contact was chosen that was located in the hippocampus and related to the MTL-P300 with the largest peak amplitude recorded in the oddball paradigm and one anterior para-hippocampal position was chosen for the data recorded during the continuous visual word recognition paradigm with the maximum AMTL-N400 peak amplitude. Because our methods cannot cleanly separate perirhinal and entorhinal generators, we use the term rhinal cortex without indicating an integrated rhinal processing stage.

Analysis of Phase-Locking and Power Changes

EEG trials were filtered in the frequency range from 2 to 48 Hz (2-Hz steps) by continuous wavelet transforms implementing Morlet wavelets of five cycles length (e.g., Daubechies, 1990). The filtered signals $w_{j,k}$ (j = time point within a trial; k = trial number) hereby result from the time convolution of original signals and the complex wavelet function. Technically, the temporal resolution for the lowest frequencies of interest, as given by the half width at half maximum of the Gaussian envelope of the Morlet wavelet (e.g., Baudin, Gabriel, & Gilbert, 1994), is 468 msec for 2 Hz, 234 msec for 4 Hz, and 156 msec for 6 Hz. To avoid edge effects the trials entering the wavelet transform were segmented from −1.5 to 2.3 sec with respect to stimulus presentation and an interval of 1.3 sec at the beginning and the end of the trials was afterwards discarded. From the wavelet transformed signals $w_{j,k}$, the phases $\varphi_{j,k}$ {$\varphi_{j,k}$ = arctan [Im($w_{j,k}$)/Re($w_{j,k}$)]} and the power values $P_{j,k}$ [$P_{j,k}$ = Re($w_{j,k}$)^2 + Im($w_{j,k}$)^2] were extracted for each time point j of each trial k. Power values were averaged separately for each condition. The calculation of inter-trial phase-locking values was done by a procedure suitable for the evaluation of small trial numbers. In contrast to phase-locking estimates based on calculations of circular variance (e.g., Fell, Klaver, et al., 2001), this method is not biased by the number of trials. For this purpose, phase distributions for target and nontarget trials were divided into eight boxes of 45° covering the range from −180° to +180°. Distribution probabilities X_i were calculated for each box i and each time point j. Phase-locking values PL_j were then evaluated based on a normalized entropy measure.

$$PL_j = 1 + \sum_{i=1}^{8} X_{i,j} * \log X_{i,j} / \log(8)$$

To allow a finer phase resolution, calculations were iterated for 45 shifts of the boxes about 1° and finally the phase-locking values resulted from the averages of these iterations. Power and phase-locking values were averaged for non-overlapping successive time windows of 100 msec duration from −200 to 1000 msec (12 windows in total). Afterwards, values were normalized with respect to the prestimulus time window from −200 to −100 msec separately for each subject and each filter frequency. Only for the graphical depiction, power and phase-locking values were transformed into dB scale ($10*\log_{10}$).

Statistical Analysis

For statistical evaluation, we conducted three-way ANOVAs with time (window) and stimulus (target vs. nontarget, hits vs. correct rejections) as repeated measures and frequency as independent variable. The p values were Huynh–Feldt corrected for inhomogeneities of covariance when necessary (Huynh & Feldt, 1976). Two-way ANOVAs were calculated separately for target and nontarget responses in the oddball paradigm and hits (correctly recognized old items) and correct rejections (correctly identified new items) in the recognition paradigm. Subsequently, two-tailed paired-sample t tests comparing target and nontarget responses, as well as hits and correct rejections, were performed for each individual time window and frequency. Of all statistically significant results of the t tests only those are reported which were extended across at least two contiguous time intervals.

REFERENCES

Basar, E. (1972). A study of the time and frequency characteristics of the potentials evoked in the acoustical cortex. *Kybernetik, 10,* 61–64.

Basar, E. (1980). *EEG brain dynamics: Relation between EEG and brain evoked potentials.* New York: Elsevier.

Basar, E., Basar-Eroglu, C., Rosen, B., & Schutt, A. (1984). A new approach to endogenous event-related potentials in man: Relation between EEG and P300-wave. *International Journal of Neuroscience, 24,* 1–21.

Baudin, F., Gabriel, A., & Gibert, D. (1994). Time/frequency analysis of solar p-modes. *Astronomy and Astrophysics, 285,* 29–32.

Bullock, T. H., McClune, M. C., Achimowicz, J. Z., Iragui-Madoz, V. J., Duckrow, R. B., & Spencer, S. S. (1995). EEG coherence has structure in the millimeter domain: Subdural and hippocampal recordings from epileptic patients. *Electroencephalography and Clinical Neurophysiology, 95,* 161–177.

Daubechies, I. (1990). The wavelet transform, time–frequency localisation and signal analysis. *IEEE Transactions on Information Theory, 36,* 961–1005.

Demiralp, T., Ademoglu, A., Istefanopulos, Y., & Gulcur, H. O. (1998). Analysis of event-related potentials (ERP) by damped sinusoids. *Biological Cybernetics, 78,* 487–493.

Donchin, E., & Coles, M. G. H. (1988). Is the P300 component a manifestation of context updating? *Behavioral and Brain Sciences, 11,* 357–374.

Elbert, T., & Rockstroh, B. (1987). Threshold regulation—A key to the understanding of the combined dynamics of EEG and event-related potentials. *Journal of Psychophysiology, 4,* 317–333.

Fell, J., Hinrichs, H., & Röschke, J. (1997). Time course of human 40 Hz EEG activity accompanying P3 responses in an auditory oddball paradigm. *Neuroscience Letters, 235,* 121–124.

Fell, J., Klaver, P., Lehnertz, K., Grunwald, T., Schaller, C., Elger, C. E., & Fernández, G. (2001). Human memory formation is accompanied by rhinal–hippocampal coupling and decoupling. *Nature Neuroscience, 4,* 1259–1264.

Fernández, G., Effern, A., Grunwald, T., Pezer, N., Lehnertz, K., Dümpelmann, M., Van Roost, D., & Elger, C. E. (1999). Real-time tracking of memory formation in the human rhinal cortex and hippocampus. *Science, 285,* 1582–1585.

Fernández, G., Heitkemper, P., Grunwald, T., Van Roost, D., Urbach, H., Pezer, N., Lehnertz, K., & Elger, C. E. (2001). An inferior temporal stream for word processing with integrated mnemonic function. *Human Brain Mapping, 14,* 251–260.

Fernández, G., Klaver, P., Fell, J., Grunwald, T., & Elger, C. E. (2002). Human declarative memory formation: Segregating rhinal and hippocampal contributions. *Hippocampus, 12,* 514–519.

Grunwald, T., Beck, H., Lehnertz, K., Blümcke I., Pezer, N., Kutas, M., Kurthen, M., Karakas, H. M., Van Roost, D., Wiestler, O. D., & Elger, C. E. (1999). Limbic P300s in temporal lobe epilepsy with and without Ammon's horn sclerosis. *European Journal of Neuroscience, 11,* 1899–1906.

Grunwald, T., Elger, C. E., Lehnertz, K., Van Roost, D., & Elger, C. E. (1995). Alterations of intrahippocampal cognitive potentials in temporal lobe epilepsy. *Electroencephalography and Clinical Neurophysiology, 95,* 53–62.

Grunwald, T., Lehnertz, K., Heinze, H. J., Helmstaedter, C., & Elger, C. E. (1998). Verbal novelty detection within the human hippocampus proper. *Proceedings of the National Academy of Sciences, U.S.A., 95,* 3193–3197.

Grunwald, T., Lehnertz, K., Helmstaedter, C., Kutas, M., Pezer, N., Kurthen, M., Van Roost, D., & Elger, C. E. (1998). Limbic ERP's predict verbal memory after left-sided hippocampectomy. *NeuroReport, 9,* 3375–3378.

Grunwald, T., Lehnertz, K., Pezer, N., Kurthen, M., Van Roost, D., Schramm, J., & Elger, C. E. (1999). Prediction of postoperative seizure control by hippocampal event-related potentials. *Epilepsia, 40,* 303–306.

Guillem, F., N'kaoua, B., Rougier, A., & Claverie, B. (1995). Effects of temporal versus temporal plus extra-temporal lobe epilepsies on hippocampal ERPs: Physiopathological implications for recognition memory studies in human. *Cognitive Brain Research, 2,* 147–153.

Halgren, E., Marinkovic, K., & Chauvel, P. (1998). Generators of the late cognitive potentials in auditory and visual oddball tasks. *Electroencephalography and Clinical Neurophysiology, 106,* 156–164.

Halgren, E., & Smith, M. E. (1987). Cognitive evoked potentials as modulatory processes in human memory formation and retrieval. *Human Neurobiology, 6,* 129–139.

Halgren, E., Squires, N. K., Wilson, C. L., Rohrbaugh, J. W., Babb, T. L., & Crandall, P. H. (1980). Endogenous potentials generated in the human hippocampal formation and amygdala by infrequent events. *Science, 210,* 803–805.

Huynh, H., & Feldt, L. S. (1976). Estimation of the box correction for degrees of freedom from sample data in the randomized plot and split plot designs. *Journal of Educational Statistics, 1,* 69–82.

Jackson, G. D., & Duncan, J. S. (1996). *MRI neuroanatomy.* New York: Churchill Livingstone.

Logothetis, N. K. (2002). The neural basis of the blood-oxygen-level-dependent functional magnetic resonance imaging signal. *Philosophical Transactions of the Royal Society London, Series B. Biological Sciences, 357,* 1003–1037.

Logothetis, N. K., Pauls, J., Augath, M., Trinath, T., & Oeltermann, A. (2001). Neurophysiological investigation of the basis of the fMRI signal. *Nature, 412,* 150–157.

Lopes da Silva, F. (1993). Event-related potentials: Methodology and quantification. In E. Niedermeyer & F. Lopes da Silva (Eds.), *Electroencephalography: Basic principles, clinical applications, and related fields,* 3rd ed. (pp. 877–886). Baltimore: Williams & Wilkins.

Makeig, S., Westerfield, M., Jung, T. P., Enghoff, S., Townsend, J., Courchesne, E., & Sejnowski, T. J. (2002). Dynamic brain sources of visual evoked responses. *Science, 295,* 690–694.

McCarthy, G., Nobre, A. C., Bentin, S., & Spencer, D. D. (1995). Language-related field potentials in the anterior–medial temporal lobe: I. Intracranial distribution and neural generators. *Journal of Neuroscience, 15,* 1080–1089.

Menon, V., Freeman, W. J., Cutillo, B. A., Desmond, J. E., Ward, M. F., Bressler, S. L., Laxer, K. D., Barbaro, N., & Gevins, A. S. (1996). Spatio-temporal correlations in human gamma band electrocorticograms. *Electroencephalography and Clinical Neurophysiology, 98,* 89–102.

Nobre, A. C., & McCarthy, G. (1995). Language-related field potentials in the anterior–medial temporal lobe: II. Effects of word type and semantic priming. *Journal of Neuroscience, 15,* 1090–1098.

Paller, K. A., McCarthy, G., Roessler, E., Allison, T., & Wood, C. C. (1992). Potentials evoked in human and monkey medial temporal lobe during auditory and visual oddball paradigms. *Electroencephalography and Clinical Neurophysiology, 84,* 269–279.

Rugg, M. D., & Nagy, M. E. (1989). Event-related potentials and recognition memory for words. *Electroencephalography and Clinical Neurophysiology, 72,* 395–406.

Sannita, W. G., Bandini, F., Beelke, M., De Carli, F., Carozzo, S., Gesino, D., Mazzella, L., Ogliastro, C., & Narici, L. (2001). Time dynamics of stimulus- and event-related gamma band activity: Contrast-VEPs and the visual P300 in man. *Clinical Neurophysiology, 112,* 2241–2249.

Sayers, B. M., Beagley, H. A., & Henshall, W. R. (1974). The mechanism of auditory evoked EEG responses. *Nature, 247,* 481–483.

Schupp, H. T., Lutzenberger, W., Rau, H., & Birbaumer, N. (1994). Positive shifts of event-related potentials: A state of cortical disfacilitation as reflected by the startle reflex probe.

Electroencephalography and Clinical Neurophysiology, 90, 135–144.

Smith, M. E., Stapleton, J. M., & Halgren, E. (1986). Human medial temporal lobe potentials evoked in memory and language tasks. *Electroencephalography and Clinical Neurophysiology, 63,* 145–159.

Van Roost, D., Solymosi, L., Schramm, J., Van Oosterwyck, B., & Elger, C. E. (1998). Depth electrode implantation in the length axis of the hippocampus for the presurgical evaluation of medial temporal lobe epilepsy: A computed tomography-based stereotactic insertion technique and its accuracy. *Neurosurgery, 43,* 819–826.

Verleger, R. (1998). Event-related potentials and cognition: A critique of the context updating hypothesis and an alternative interpretation of P3. *Behavioral and Brain Sciences, 11,* 343–427.

Yordanova, J., & Kolev, V. (1998). Single-sweep analysis of the theta frequency band during an auditory oddball task. *Psychophysiology, 35,* 116–126.